论著·基础医学

芍药苷通过调控PI3K/AKT/HIF-1α通路减轻脂多糖诱导的HK-2细胞有氧糖酵解

谢 菁[1],李若男[1],高慧慧[1],杨顺凯[1],马玉清[2] 兰州大学:[1]第一临床医学院,[2]第一医院麻醉科,甘肃兰州

［**摘要**］ **目的** 探讨芍药苷(paeoniflorin,PF)对脂多糖(lipopolysaccharide,LPS)诱导的肾小管上皮细胞(HK-2细胞)有氧糖酵解的影响及其作用机制。**方法** 本研究分为预实验和正式实验两部分。①预实验:体外培养HK-2细胞,CCK-8实验检测细胞活力,RT-qPCR检测炎症因子mRNA的水平,进行LPS最佳造模浓度筛选、芍药苷毒性实验和浓度筛选。正式实验:将HK-2细胞分成对照组(CON组)、LPS组、LPS+PF组和LPS+PF+740Y-P组。通过建立LPS诱导的SA-AKI肾小管细胞损伤的体外模型,分别给予PF和PI3K激活剂740Y-P干预,造模24 h后取材,CCK-8实验检测细胞活力;细胞外酸化率(extra cellular acidification rate,ECAR)试剂盒检测ECAR;ELISA检测IL-1β、IL-18、乳酸(lactic acid,Lac)以及乳酸脱氢酶A(lactate dehydrogenase A,LDHA);Western blot检测p-PI3K、p-AKT、HIF-1α、丙酮酸激酶2(pyruvate kinase 2,PKM2)、NOD样受体热蛋白结构域相关蛋白3(NOD-like receptor thermal protein domain associated protein 3,NLRP3)的表达;免疫荧光观察有氧糖酵解关键酶PKM2的表达和分布情况。**结果** ①筛选出LPS最佳造模浓度为20.0 μg/mL,芍药苷安全剂量为0~100.0 μmol/L,芍药苷的最佳治疗浓度为25.0 μmol/L。②与CON组相比,LPS组细胞活力明显下降(P<0.05),ECAR明显升高(P<0.05),IL-1β、IL-18、Lac、LDHA水平明显增加(P<0.05),p-PI3K、p-AKT、HIF-1α、p-PKM2、NLRP3蛋白相对表达量明显增加(P<0.05),细胞核内PKM2荧光强度明显增强(P<0.05)。与LPS组相比,LPS+PF组ECAR明显下降(P<0.05),IL-1β、IL-18、Lac、LDHA水平明显下降(P<0.05),p-PI3K、p-AKT、HIF-1α、p-PKM2、NLRP3蛋白相对表达量明显减少(P<0.05),细胞核内PKM2荧光强度明显减弱(P<0.05)。与LPS+PF组相比,LPS+PF+740Y-P组ECAR明显升高(P<0.05),IL-1β、IL-18、Lac、LDHA水平明显增加(P<0.05),p-PI3K、p-AKT、HIF-1α、p-PKM2、NLRP3蛋白相对表达量明显增加(P<0.05),细胞核内PKM2荧光强度明显增强(P<0.05)。**结论** 芍药苷通过抑制PI3K/AKT/HIF-1α信号通路,降低HK-2细胞有氧糖酵解水平,减轻炎症反应。

［**关键词**］ 脓毒症相关急性肾损伤;有氧糖酵解;PI3K/AKT/HIF-1α通路;芍药苷;肾小管上皮细胞
［**中图法分类号**］ R285.5;R329.26;R692.6 ［**文献标志码**］ A

Paeoniflorin alleviates LPS-induced aerobic glycolysis in HK-2 cells by modulating the PI3K/AKT/HIF-1α pathway

XIE Jing[1], LI Ruonan[1], GAO Huihui[1], YANG Shunkai[1], MA Yuqing[2] [1]First School of Clinical Medicine, Lanzhou University, Lanzhou, Gansu; [2]Department of Anesthesiology, the First Hospital of Lanzhou University, Lanzhou, Gansu, China

［**Abstract**］ **Objective** To investigate the effects of paeoniflorin (PF) on lipopolysaccharide (LPS)-induced aerobic glycolysis in renal tubular epithelial cell line HK-2 and its underlying mechanism of action.

［**基金项目**］ 甘肃省自然科学基金面上项目(24JRRA1075);兰州大学第一医院院内基金(ldyyyn2022-5)
［**通信作者**］ 马玉清,E-mail:myq2392466@163.com

2097-0927/Copyright © 2025, 陆军军医大学(第三军医大学)。这篇开放获取文章遵循 CC BY 许可协议 (https://creativecommons.org/licenses/by/4.0/)
引用格式:谢菁,李若男,高慧慧,等. 芍药苷通过调控PI3K/AKT/HIF-1α通路减轻脂多糖诱导的HK-2细胞有氧糖酵解[J]. 陆军军医大学学报,2025,47(20):2483-2494. DOI:10.16016/j.2097-0927.202505035.
Citation: XIE J, LI R N, GAO H H, *et al*. Paeoniflorin alleviates LPS-induced aerobic glycolysis in HK-2 cells by modulating the PI3K/AKT/HIF-1α pathway [J]. J Army Med Univ, 2025, 47(20): 2483-2494. DOI: 10.16016/j.2097-0927.202505035.

Methods This study consists of a preliminary experiment and a formal experiment. Preliminary experiment: CCK-8 assay and RT-qPCR were used respectively to measure cell viability and mRNA expression levels of inflammatory factors in HK-2 cells after LPS stimulation to determine the optimal LPS concentration for modeling as well as to evaluate the toxicity of PF and screen for its appropriate concentration. Formal experiment: HK-2 cells were divided into control group (CON group), LPS group, LPS+PF group and LPS+PF+740Y-P group. LPS was used to establish a cell model of sepsis associated-acute kidney injury (SA-AKI) in HK-2 cells, and then the cell model was treated with PF and PI3K activator 740Y-P, correspondingly for 24 h. CCK-8 assay was employed to detect cell viability, and Extracellular Acidification Rate (ECAR) Kit was utilized to measure the rate. The contents of IL-1β, IL-18, lactic acid (Lac) and lactate dehydrogenase A (LDHA) were determined with ELISA. Western blotting was applied to detect the expression of p-PI3K, p-AKT, HIF-1α, pyruvate kinase 2 (PKM2, a key enzyme in aerobic glycolysis) and NOD-like receptor thermal protein domain associated protein 3 (NLRP3), and immunofluorescence assay was performed to observe the expression and distribution of PKM2. **Results** ① Our preliminary experiment identified that the optimal concentration of LPS for modeling was 20.0 μg/mL, a safe dosage range of PF was 0~100.0 μmol/L, and its optimal therapeutic concentration was 25.0 μmol/L. ② Compared with the CON group, LPS stimulation resulted in significantly decreased cell viability ($P<0.05$), increased ECAR ($P<0.05$), elevated contents of IL-1β, IL-18, Lac and LDHA ($P<0.05$), up-regulated protein levels of p-PI3K, p-AKT, HIF-1α, p-PKM2 and NLRP3 ($P<0.05$), and enhanced fluorescence intensity of PKM2 in the nucleus of cells ($P<0.05$). Compared with the model group, PF treatment reversed all above effects induced by LPS stimulation (all $P<0.05$). Compared with the LPS+PF group, in the LPS+PF+740Y-P group, ECAR was elevated ($P<0.05$), the contents of IL-1β, IL-18, Lac and LDHA were increased ($P<0.05$), and the relative expression levels of p-PI3K, p-AKT, HIF-1α, p-PKM2 and NLRP3 were increased ($P<0.05$), and the fluorescence intensity of PKM2 was strengthened ($P<0.05$) and enhanced in the nucleus ($P<0.05$). **Conclusion** PF reduces aerobic glycolysis in HK-2 cells and alleviates the inflammatory response by inhibiting the PI3K/AKT/HIF-1α signaling pathway.

[**Key words**] sepsis associated-acute kidney injury; aerobic glycolysis; PI3K/AKT/HIF-1α pathway; paeoniflorin; renal tubular epithelial cells

Supported by the General Project of Natural Science Foundation of Gansu Province (24JRRA1075) and the Fund of the First Hospital of Lanzhou University (ldyyyn2022-5). Corresponding author: MA Yuqing, E-mail: myq2392466@163.com

脓毒症相关急性肾损伤(sepsis associated-acute kidney injury,SA-AKI)是脓毒症多器官功能障碍中一种常见且严重的并发症[1]。据统计,60%的AKI是由严重脓毒症引起[2],与非脓毒症所致肾损伤患者相比,SA-AKI患者的临床预后明显更差[3],病死率高达30%~70%[4]。研究表明,SA-AKI发病机制与肾小管上皮细胞、巨噬细胞、血管内皮细胞等多种细胞的损伤和功能障碍有关,有氧糖酵解和炎症反应也参与SA-AKI的发生发展[4-6]。

在细胞免疫应答过程中,有氧糖酵解发挥着关键调控作用,是炎症性疾病治疗的新靶点[7]。SA-AKI患者发生有氧糖酵解时,炎症反应显著加剧[8]。体内外实验研究发现,在盲肠结扎穿刺(cecal ligation and puncture, CLP)诱导的脓毒症小鼠模型和脂多糖(LPS)刺激HK-2细胞构建的SA-AKI体外模型中,有氧糖酵解终产物及其限速酶的表达上调,特异性抑制有氧糖酵解通路可有效缓解SA-AKI的发展进程[9-10]。

PI3K/AKT信号通路参与有氧糖酵解的发生[11-12],激活PI3K/AKT通路能够上调HIF-1α的表达[13]。HIF-1α作为关键的转录调控因子,可特异性结合有氧糖酵解关键酶如丙酮酸激酶M2亚型(pyruvate kinase 2, PKM2)和乳酸脱氢酶A(lactate dehydrogenase A, LDHA)的启动子区域,直接调控其转录表达[14]。但PI3K/AKT/HIF-1α通路是否参与SA-AKI的有氧糖酵解尚无研究。

芍药苷(paeoniflorin,PF)是一种单萜双环苷类化合物,是中药白芍和赤芍的主要活性成分,具有抗炎、免疫调节等作用。XIE等[15]发现,PF通过PI3K/AKT

通路抑制LPS诱导的小鼠单核巨噬细胞炎症反应,但PF能否抑制HK-2细胞有氧糖酵解和炎症反应尚待探究。因此,本研究采用LPS诱导HK-2细胞,建立SA-AKI肾小管细胞损伤的体外模型,探讨PF是否通过调控PI3K/AKT/HIF-1α信号通路,减轻有氧糖酵解和炎症反应。

1 材料与方法

1.1 实验细胞和试剂

人来源的肾小管上皮细胞HK-2购自武汉普诺赛生命科技有限公司。LPS、芍药苷购自美国MCE公司,PI3K特异性激动剂740Y-P购自美国Glpbio公司,IL-1β、IL-18、乳酸(lactic acid,Lac)、LDHA的酶联免疫吸附(ELISA)测定试剂盒购自江苏酶免实业有限公司,细胞外酸化率(extra cellular acidification rate,ECAR)荧光法测试盒购自武汉伊莱瑞特生物科技股份有限公司,反转录试剂盒、荧光定量试剂盒购自上海翌圣生物科技有限公司,p-PI3K、PI3K、p-AKT、AKT、HIF-1α、p-PKM2、PKM2抗体购自美国ImmunoWay公司,NOD样受体热蛋白结构域相关蛋白3(NOD-like receptor thermal protein domain associated protein 3,NLRP3)抗体购自美国proteintech公司,Actin抗体购于美国GeneTex公司。

1.2 方法

1.2.1 LPS最佳造模浓度、芍药苷毒性实验及其浓度筛选 将HK-2细胞用含10%FBS、1%青霉素-链霉素的MEM培养基,在37 ℃、5%CO_2培养箱中进行培养。待HK-2细胞融合度达到80%时:①筛选LPS最佳造模浓度:分别用不同浓度(0.5、1.0、2.0、5.0、10.0、20.0、40.0 μg/mL)LPS处理24 h,以未处理的细胞作为对照,CCK-8实验检测细胞活力,RT-qPCR检测炎症因子mRNA的水平,筛选LPS最佳造模浓度。②芍药苷毒性实验:分别用不同浓度(12.5、25.0、50.0、100.0、200.0 μmol/L)PF处理HK-2细胞24 h,以未处理的细胞作为对照,CCK-8实验检测细胞活力,以评估PF对细胞的毒性作用,确定PF的安全剂量范围。③筛选芍药苷最佳治疗浓度:分为CON组、LPS组、LPS+DMSO组、LPS+PF(12.5 μmol/L)组、LPS+PF(25.0 μmol/L)组、LPS+PF(50.0 μmol/L)组、LPS+PF(100.0 μmol/L)组。其中CON组为未处理的细胞;LPS组用20.0 μg/mL的LPS处理HK-2细胞24 h;LPS+DMSO组作为溶剂对照组,同时加入20.0 μg/mL的LPS,及与LPS等体积的0.1%DMSO处理HK-2细胞24 h;LPS+PF各组用不同浓度(0~100.0 μmol/L)PF处理HK-2细胞4 h后,再给予LPS(20.0 μg/mL)处理24 h,CCK-8实验检测细胞活力,RT-qPCR检测炎症因子mRNA的水平,筛选PF最佳治疗剂量。

1.2.2 正式实验分组 将HK-2细胞分为对照(CON)组、LPS组、LPS+芍药苷(LPS+PF)组、LPS+芍药苷+PI3K激活剂740Y-P(LPS+PF+740Y-P)组。CON组为未处理的细胞;LPS组给予20.0 μg/mL LPS处理24 h;LPS+PF组用25.0 μmol/L PF预处理4 h后,再加入20.0 μg/mL LPS处理24 h;LPS+PF+740Y-P组先用25.0 μmol/L PF和20.0 μmol/L 740Y-P[16]共同预处理4 h后,再加入20.0 μg/mL LPS处理24 h。

1.2.3 CCK-8实验检测细胞活力 将HK-2细胞按照每孔5 000个接种于96孔板中,空白组加入与LPS等体积的PBS,药物组分别给予不同浓度的LPS、PF(按照1.2.1的给药剂量及处理时间),每个浓度设置5个复孔处理24 h,每孔加入10 μL CCK-8染色液,在37 ℃、5%CO_2细胞培养箱中孵育1 h后,利用酶标仪在450 nm处测定光密度值[D(450)],并计算细胞活力:

$$细胞活力(\%)=\frac{D_{药物组}-D_{空白组}}{D_{对照组}-D_{空白组}}\times 100\%。$$

1.2.4 RT-qPCR 按照1.2.1的给药剂量及处理时间予以HK-2细胞药物处理后,收集细胞样本,Trizol试剂提取总RNA,使用反转录试剂盒合成cDNA。通过PCR扩增仪(A300,杭州朗基科学仪器有限公司)、荧光定量PCR仪[201901003,鲲鹏基因(北京)科学仪器有限公司]检测完成RT-qPCR过程。目标基因引物序列见表1。

表1 目标基因引物序列

Table 1 Primer sequences of target genes

Gene	Primer sequences
IL-1β	Upstream: 5′-AGAAGTACCTGAGCTCGCCA-3′
	Downstream: 5′-GTCCATGGCCACAACAACTG-3′
IL-18	Upstream: 5′-CCTCAGACCTTCCAGATCGC-3′
	Downstream: 5′-GGTCCGGGGTGCATTATCTC-3′
β-actin	Upstream: 5′-AACCGCGAGAAGATGACCCA-3′
	Downstream: 5′-GAGGTAGTCAGTCAGGTCCC-3′

1.2.5 ECAR试剂盒检测ECAR变化 本测试盒使用特异性的探针(Ex/Em:490 nm/535 nm),当细胞外环境的pH发生变化时,探针的荧光值也会相应发生变化。发生酸化的细胞外环境会使探针的荧光值降低,以此来检测细胞外的酸化率。设计测定孔和空

白孔,将细胞接种至96孔黑色透底酶标板孔中,接种细胞密度为2×10^5/mL,每孔100 μL细胞悬液。细胞接种完毕放入37 ℃、5%CO_2培养箱,静置培养过夜后,去除细胞培养液,每孔加入100 μL试剂1;空白孔为不接种细胞的孔。根据实验设计加入相应药物刺激细胞,药物干预完成后,进行下一步实验。接种后细胞,37 ℃避光孵育30 min,同时将荧光酶标仪温度设置为37 ℃。向各孔中加入100 μL工作液,荧光酶标仪于激发波长490 nm、发射波长535 nm处检测各孔荧光值,每隔2~3分钟检测一次,总时间100~120 min,绘制荧光值随时间变化的曲线图,选择线性段计算细胞外酸化率(ECAR):ECAR =($\Delta F_{测定}-\Delta F_{空白}$)/ΔT。其中$\Delta F_{测定}$指测定孔变化荧光值(F1-F2);$\Delta F_{空白}$指空白孔变化荧光值(F1-F2);ΔT指荧光值变化时间(T2-T1)。

1.2.6 ELISA法检测乳酸(Lac)、乳酸脱氢酶(LDHA)、IL-1β、IL-18水平 收集各组细胞的上清液,按照ELISA试剂盒操作说明书配制试剂和操作。使用酶标仪在450 nm波长处依次读取各孔光密度值[*D*(450)]。绘制标准曲线,计算各组细胞上清中LDHA、Lac、IL-1β、IL-18的含量。

1.2.7 Western blot检测蛋白表达水平 收集各组细胞,加入含有蛋白酶和磷酸酶抑制剂的裂解液4 ℃充分裂解细胞,以12 000×*g*离心10 min,取上清。蛋白质定量后,取20 μg蛋白上样进行凝胶电泳分离,转至PVDF膜上。5%脱脂奶粉室温封闭4 ℃过夜,分别加入p-PI3K、PI3K、p-AKT、AKT、HIF-1α、p-PKM2、PKM2、NLRP3、β-actin抗体室温孵育1 h。加入二抗羊抗兔IgG(1∶20 000),室温孵育1 h。采用Image J量化条带灰度值,目标蛋白和内参蛋白灰度比值反映蛋白表达量。

1.2.8 免疫荧光检测 将HK-2细胞经爬片种板处理后,PBS清洗,4%多聚甲醛(500 μL/孔)固定15 min,PBS漂洗3次。0.5% Triton X-100(PBS配制)室温通透5 min。PBS浸洗3次(3 min/次),3% BSA(200 μL/孔)37 ℃封闭30 min。一抗(PKM2,1∶200,200 μL/孔)4 ℃过夜孵育,PBS清洗3次(7 min/次)。二抗(山羊抗兔IgG,1∶1 000,500 μL/孔)37 ℃避光孵育1 h,PBS清洗3次(7 min/次)。DAPI染核5 min,PBS清洗3次(5 min/次)。封片后荧光显微镜观察并拍照,使用Image J对图片进行定量,统计平均荧光强度。

1.2.9 统计学分析 采用SPSS 22.0软件对数据进行统计学分析,采用Graphpad Prism 10.0软件作图。符合正态分布的计量资料以$\bar{x}\pm s$表示,多组间比较采用单因素方差分析,两组间比较采用LSD-*t*检验。*P*<0.05为差异具有统计学意义。

2 结果

2.1 LPS浓度、芍药苷毒性实验及其浓度筛选

2.1.1 筛选LPS最佳造模浓度 与CON组比较,不同浓度LPS干预HK-2细胞24 h后,5.0~40.0 μg/mL LPS对细胞活力有明显影响(*P*<0.05,图1A),并呈剂量依赖性下降趋势。与CON组比较,不同浓度LPS干预HK-2细胞24 h后,10.0~40.0 μg/mL LPS组IL-1β、IL-18 mRNA水平明显升高(*P*<0.05,图1B、C)。结合CCK-8实验和RT-qPCR结果,选择20.0 μg/mL LPS作为最佳造模浓度。

2.1.2 芍药苷(PF)毒性实验 与CON组比较,芍药苷干预24 h后,除200.0 μmol/L的PF显著降低细胞活力(*P*<0.05),其余不同浓度的芍药苷对细胞活力无明显影响(图1D)。因此确定PF安全药物浓度为0~100.0 μmol/L。

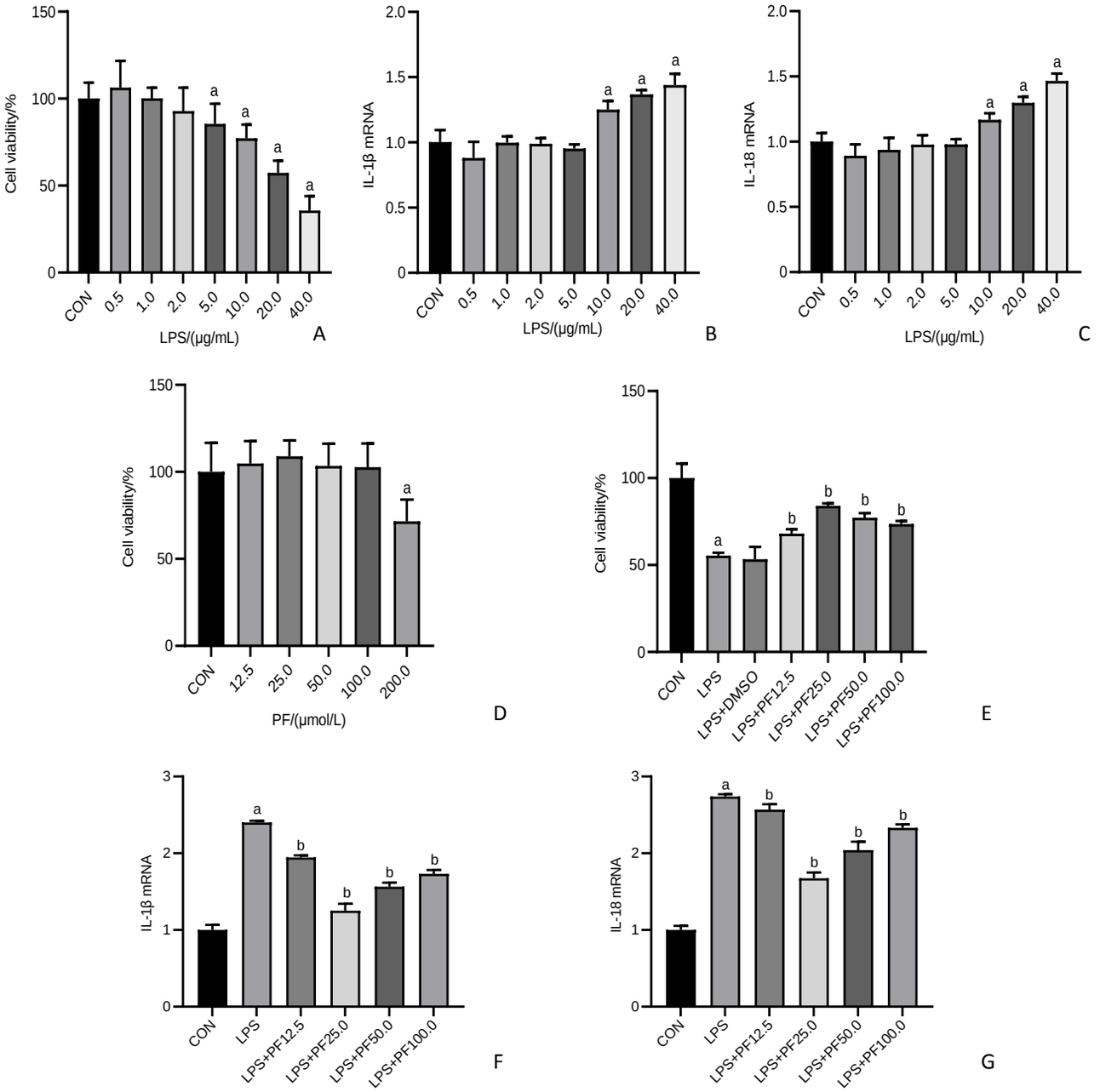
2.1.3 筛选芍药苷(PF)最佳治疗剂量 与CON组比较,LPS组明显降低细胞活力(*P*<0.05);与LPS组比较,不同浓度PF处理后,细胞活力有不同程度的增加(*P*<0.05)。其中,LPS+PF(25.0 μmol/L)组细胞活力最高(*P*<0.05),见图1E。与CON组比较,LPS组IL-1β、IL-18 mRNA水平明显升高(*P*<0.05),见图1B、C。与LPS组比较,不同浓度PF处理后,IL-1β、IL-18 mRNA水平明显下降(*P*<0.05),其中LPS+PF(25.0 μmol/L)组炎症因子mRNA水平下降最明显,故选择25.0 μmol/L作为PF的最佳治疗剂量,见图1F、G。

2.2 PF可降低LPS引起的细胞外酸化率升高

在相同时间段内,与CON组比较,LPS组荧光值降低,细胞外酸化率明显升高(*P*<0.05);与LPS组比较,LPS+PF组荧光值明显升高,细胞外酸化率明显下降(*P*<0.05);与LPS+PF组比较,LPS+PF+740Y-P组荧光值明显降低,细胞外酸化率明显升高(*P*<0.05),见图2。

2.3 PF可降低LPS引起的有氧糖酵解水平及炎症因子含量的升高

与CON组比较,LPS组LDHA、Lac、IL-1β、IL-18表达明显增加(*P*<0.05);与LPS组比较,LPS+PF组LDHA、Lac、IL-1β、IL-18表达明显减少(*P*<0.05);与LPS+PF组比较,LPS+PF+740Y-P组LDHA、Lac、IL-1β、



A、D、E: CCK-8 assay showing the effects of different concentrations of LPS (A), PF (D) and their combined treatment (E) on cell viability; B and C: Relative mRNA levels of inflammatory factors IL-1β (B) and IL-18 (C) after stimulation of different concentrations of LPS in HK-2 cells; F and G: Relative mRNA levels of IL-1β (F) and IL-18 (G) after stimulation of LPS and different concentrations of PF in HK-2 cells. LPS: Lipopolysaccharide; PF: Paeoniflorin. a: $P<0.05$, compared with the CON group; b: $P<0.05$, compared with the LPS group

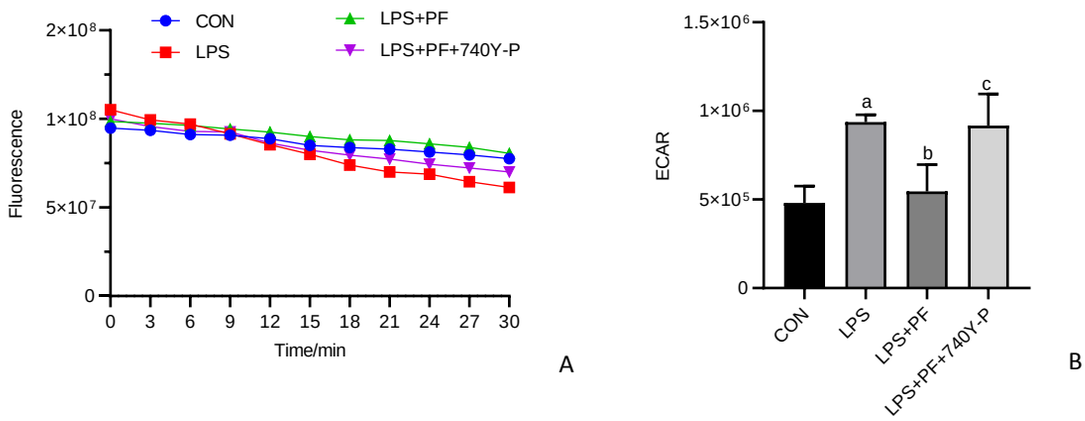
图1 细胞处理条件的筛选及联合处理后HK-2细胞炎症因子表达水平检测

Figure 1 Screening of cell treatment conditions and detection of expression levels of inflammatory factors in HK-2 cells after LPS and combined treatment

IL-18表达明显增加($P<0.05$),见图3。

2.4 PF可降低LPS引起的NLRP3蛋白表达升高

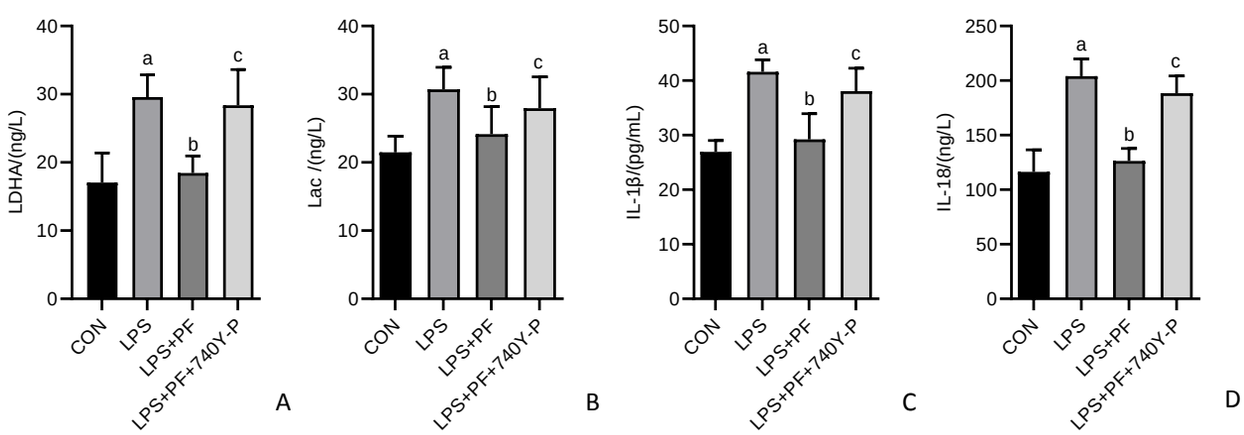
与CON组比较,LPS组NLRP3蛋白相对表达量显著升高($P<0.05$);与LPS组比较,LPS+PF组NLRP3蛋白相对表达量显著下降($P<0.05$);与LPS+PF组比较,LPS+PF+740Y-P组NLRP3蛋白相对表达量显著升高



A: Changes in fluorescence values in each group detected by ECAR kit; B: Changes of ECAR in each group. a: $P<0.05$, compared with the CON group; b: $P<0.05$, compared with the LPS group; c: $P<0.05$, compared with the LPS+PF group

图2 PF对HK-2细胞ECAR的影响

Figure 2 Effect of paeoniflorin (PF) on extra cellular acidification rate (ECAR) in HK-2 cells



a: $P<0.05$, compared with the CON group; b: $P<0.05$, compared with the LPS group; c: $P<0.05$, compared with the LPS+PF group

图3 PF对HK-2细胞有氧糖酵解指标LDHA(A)、Lac(B)及炎症因子IL-1β(C)、IL-18(D)的影响

Figure 3 Effects of paeoniflorin (PF) on aerobic glycolytic indicators lactate dehydrogenase (LDHA, as shown in A) and lactic acid (Lac, as shown in B), and on inflammatory factors IL-1β (C) and IL-18 (D) in HK-2 cells

($P<0.05$),见图4。

2.5 PF可抑制LPS引起的PI3K/AKT/HIF-1α通路的激活

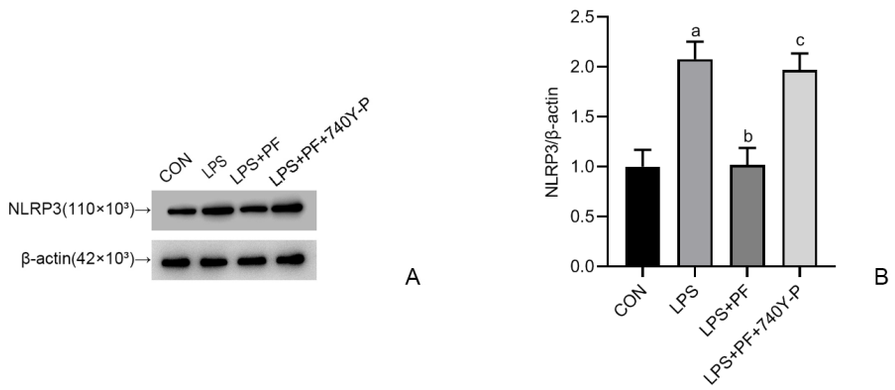
与CON组比较,LPS组p-PI3K、p-AKT及HIF-1α蛋白相对表达量显著增多($P<0.05$);与LPS组比较,LPS+PF组p-PI3K、p-AKT及HIF-1α蛋白相对表达量显著减少($P<0.05$);与LPS+PF组比较,LPS+PF+740Y-P组p-PI3K、p-AKT及HIF-1α蛋白相对表达量显著增多($P<0.05$),见图5。

2.6 PF可降低LPS引起的PKM2蛋白表达升高

与CON组比较,LPS组p-PKM2蛋白相对表达量显著升高($P<0.05$);与LPS组比较,LPS+PF组p-PKM2蛋白相对表达量显著下降($P<0.05$);与LPS+PF组比较,LPS+PF+740Y-P组p-PKM2蛋白相对表达量显著升高($P<0.05$),见图6。

2.7 PF可降低LPS引起的细胞核PKM2表达上调

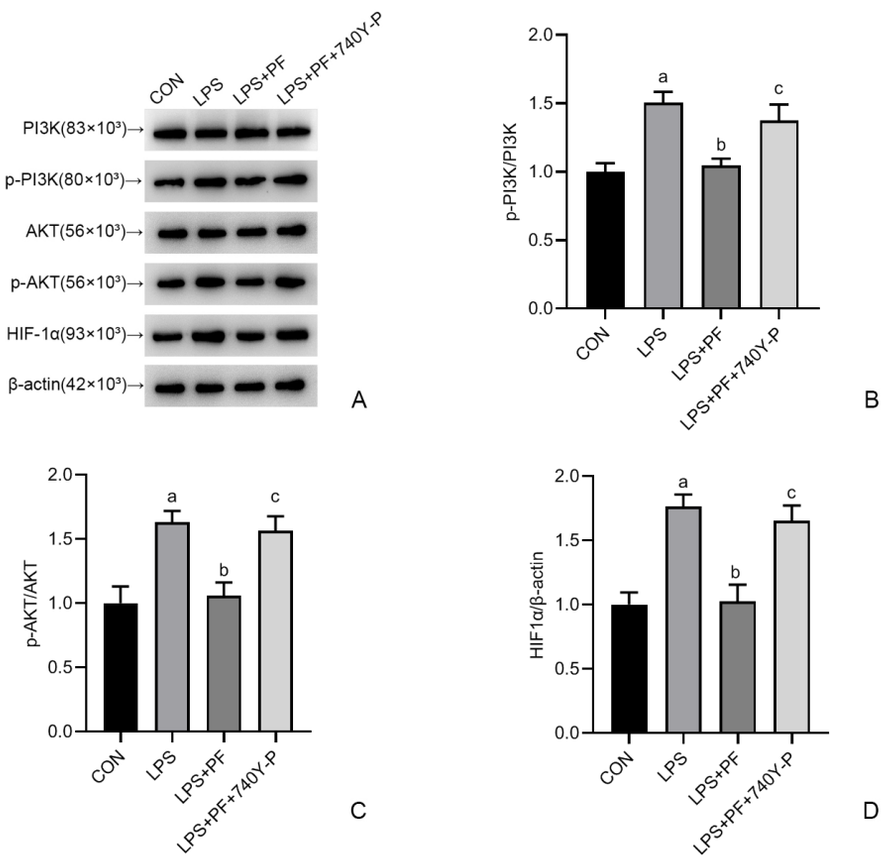
与CON组比较,LPS组免疫荧光显示PKM2表达明显上调($P<0.05$),且胞质与胞核中呈现不同程度的分布,大多数PKM2定位于细胞核内,细胞质内PKM2分布相对较少;与LPS组比较,LPS+PF组免疫荧光显示PKM2表达明显下调($P<0.05$),定位于细胞核内的PKM2显著减少,细胞质内PKM2分布相对增多;与LPS+PF组比较,LPS+PF+740Y-P组免疫荧光显示PKM2表达明显上调($P<0.05$),定位于细胞核内的



A: Western blotting results of NLRP3 in each group; B: Relative expression level of NLRP3 protein. a: $P<0.05$, compared with the CON group; b: $P<0.05$, compared with the LPS group; c: $P<0.05$, compared with the LPS+PF group

图4 PF对HK-2细胞NLRP3蛋白表达的影响

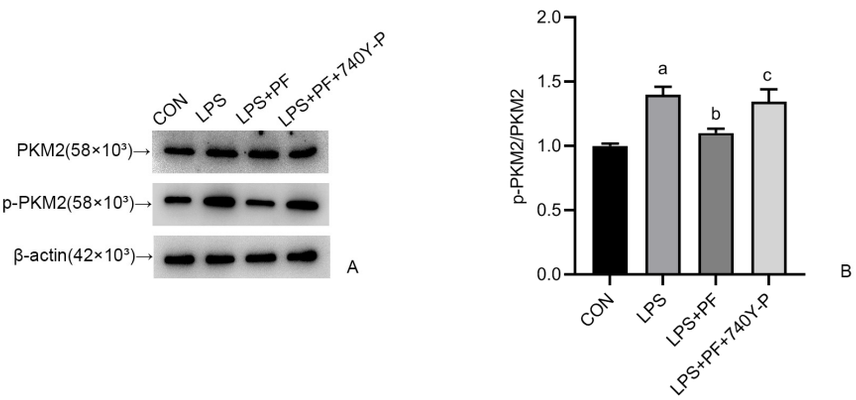
Figure 4 Effect of paeoniflorin (PF) on the expression of NLRP3 protein in HK-2 cells



A: Western blotting results of the pathway proteins in each group; B~D: Relative expression levels of p-PI3K (B), p-AKT (C) and HIF-1α (D). a: $P<0.05$, compared with the CON group; b: $P<0.05$, compared with the LPS group; c: $P<0.05$, compared with the LPS+PF group

图5 PF对HK-2细胞PI3K/AKT/HIF-1α通路的影响

Figure 5 Effect of paeoniflorin (PF) on the PI3K/AKT/HIF-1α pathway in HK-2 cells



A: Western blotting results of PKM2 and p-PKM2 in each group; B: Relative expression levels of p-PKM2 protein. a: $P<0.05$, compared with the CON group; b: $P<0.05$, compared with the LPS group; c: $P<0.05$, compared with the LPS+PF group

图6 PF对HK-2细胞PKM2蛋白表达的影响

Figure 6 Effect of paeoniflorin (PF) on the expression of PKM2 protein in HK-2 cells

PKM2显著增多,细胞质内PKM2分布相对减少,见图7。

3 讨论

本研究以HK-2细胞作为研究对象,使用LPS建立SA-AKI肾小管细胞损伤的体外模型。采用CCK-8实验评估细胞活力,RT-qPCR法检测炎症因子IL-1β、IL-18的mRNA水平,以筛选LPS最佳造模剂量。LPS造模24 h后,HK-2细胞炎症因子IL-1β、IL-18、有氧糖酵解关键酶PKM2、LDHA及其产物Lac表达上调,ECAR明显升高,证明SA-AKI肾小管细胞损伤的体外模型成功建立。

本实验在筛选PF的最佳治疗剂量时,发现50.0、100.0 μmol/L的治疗效果较25.0 μmol/L差,考虑可能是PF在培养基中的溶解度或细胞摄取机制(如转运蛋白)在25.0 μmol/L时已达饱和,更高浓度可能导致药物聚集或非特异性结合,降低了生物利用度。

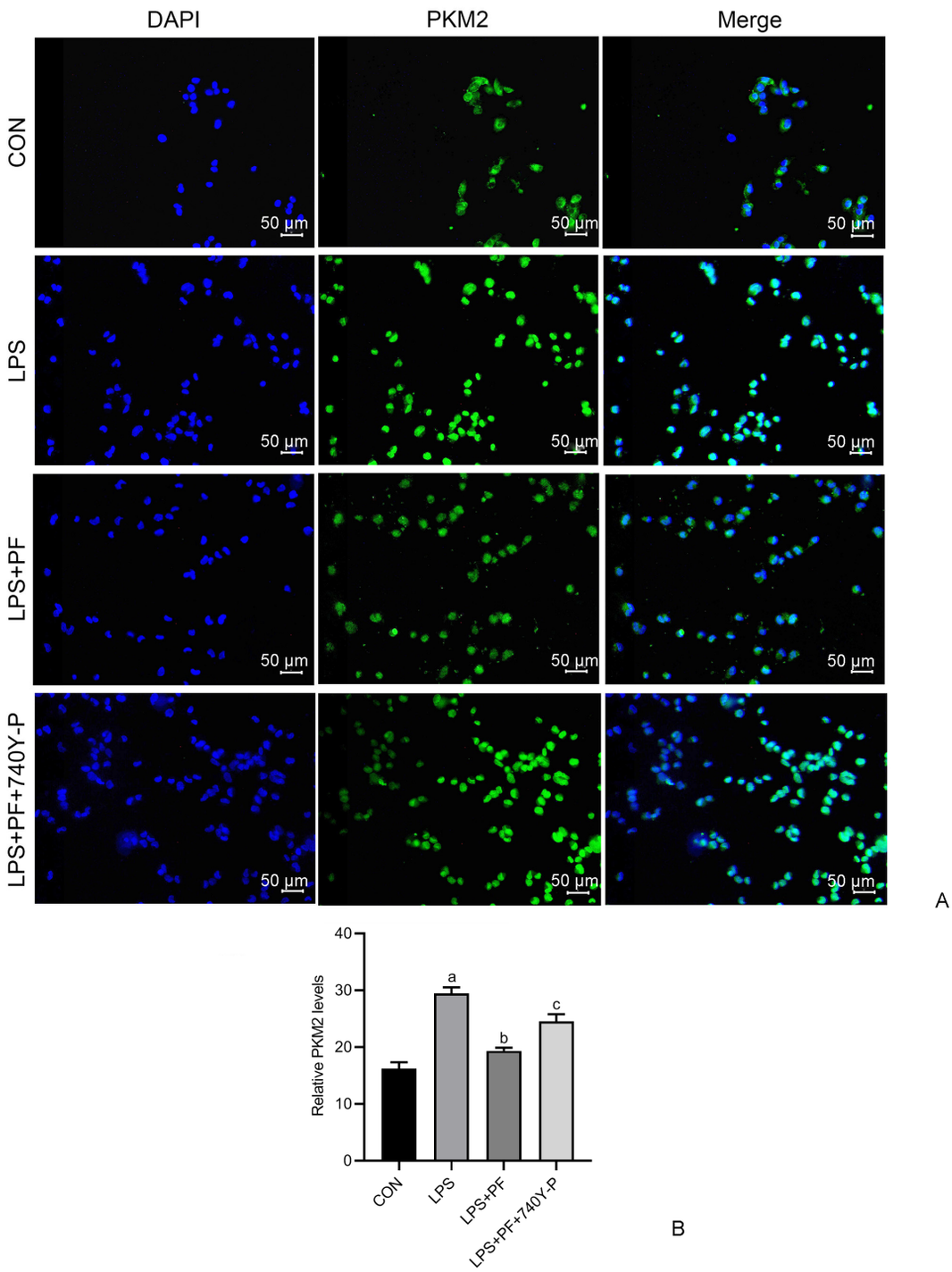
3.1 脓毒症期间代谢重编程具有细胞特异性,HK-2细胞代谢模式呈现阶段性变化

在脓毒症期间,细胞能量代谢从氧化磷酸化转变为糖酵解,这种现象被称为代谢重编程[17]。研究表明,在脓毒症引起的多器官损伤中,由Toll样受体(Toll like receptors,TLRs)介导的先天免疫和炎症反应发挥关键作用[18-20],TLR涉及代谢重编程的调控[21]。值得注意的是,脓毒症期间代谢重编程并非涉及所有细胞,而是具有细胞类型特异性。研究发现,TLR配体(如革兰阴性菌的脂多糖LPS)可诱导巨噬细胞[22]、树突状细胞[20-22]和淋巴细胞[23]的代谢转换,从氧化磷酸化转变为有氧糖酵解。心肌细胞虽仍依赖氧化磷酸化,但可能因全身缺氧或微循环障碍导致功能抑制[24]。

研究发现,脓毒症期间肾小管上皮细胞的代谢变化呈现阶段性特征[25],在早期阶段,由于肾脏微循环障碍导致的缺氧以及TNF-α等炎症信号激活HIF-1α,促使糖酵解增强,糖酵解酶表达上调;同时,内毒素(LPS)、活性氧(ROS)和钙超载引起线粒体功能障碍,导致电子传递链受损和ATP合成减少。进入后期阶段,肉碱棕榈酰转移酶1(carnitine palmitoyltransferase1,CPT1)等关键酶表达下调,脂肪酸氧化(fatty acid oxidation,FAO)受到抑制,脂肪酸供能减少,从而加剧能量危机;此时细胞通过激活自噬途径降解受损线粒体(线粒体自噬)来维持能量平衡,但过度激活的自噬可能进一步导致细胞凋亡或坏死。

3.2 PF可通过抑制有氧糖酵解缓解SA-AKI肾小管上皮细胞损伤

PKM2通过调控有氧糖酵解影响脓毒症的炎症反应[26-27]。PKM2是有氧糖酵解的关键酶,存在二聚体或四聚体两种活性形式。二聚体状态时,其催化活性降低,PKM2以二聚体形式发生核转位后,可与转录因子HIF-1α相互作用,协同激活HIF-1α下游靶基因[如葡萄糖转运蛋白1(glucose transporter 1,GLUT1)、LDHA等]的转录表达,这种调控作用显著促进有氧糖酵解的发生,形成正反馈[28]。LDHA作为糖酵解途径最后一步的关键酶,催化丙酮酸生成乳酸[29]。乳酸是有氧糖酵解过程中的关键代谢产物,可以反映细胞代



A: Expression and distribution of PKM2 in each group by immunofluorescence assay; B: Relative expression level of PKM2 in the nucleus. a: $P<0.05$, compared with the CON group; b: $P<0.05$, compared with the LPS group; c: $P<0.05$, compared with the LPS+PF group

图7 PF对HK-2细胞PKM2的表达及其分布情况的影响

Figure 7 Effect of paeoniflorin (PF) on the expression and distribution of PKM2 in HK-2 cells

谢水平[30],且乳酸增加直接促进SA-AKI的发展进程[31]。因此本研究选择PKM2、LDHA、Lac作为评估有氧糖酵解发生的指标。

本研究结果显示,LPS组p-PKM2蛋白表达上调,给予PF处理后,p-PKM2蛋白表达下调。采用免疫荧光检测HK-2细胞PKM2的表达及分布情况,结果发

现,LPS组PKM2的荧光强度在细胞核内显著增强,经过PF处理后,其荧光强度明显减弱,因此推测PF可能通过调控PKM2核转位影响有氧糖酵解。同时发现,LPS组ECAR升高,有氧糖酵解关键酶LDHA、终产物Lac水平上升;给予PF处理后,HK-2细胞ECAR降低,LDHA、Lac水平下降。AN等[31]研究表明,在CLP诱导的SA-AKI小鼠模型和LPS刺激的HK-2细胞中,乳酸产生增加。在LPS诱导的脓毒症小鼠模型中,PF可以通过上调SIRT1表达,抑制PKM2介导的有氧糖酵解[32]。PF可以下调PKM2和LDHA的表达,减少巨噬细胞乳酸分泌,降低有氧糖酵解水平[33]。这些研究发现与本实验结果高度一致。因此,在SA-AKI肾小管细胞损伤的体外模型中,PF可以一定程度地抑制有氧糖酵解。

3.3 PF可通过抑制有氧糖酵解减轻LPS诱导的HK-2细胞炎症反应

有氧糖酵解会影响NLRP3炎症小体的激活[34],NLRP3炎症小体激活后,介导IL-1β和IL-18的成熟和释放,导致炎症级联反应[35]。限制有氧糖酵解可减少脓毒症早期炎症因子释放,减轻炎症反应[36-37]。本研究发现,给予PF处理后,有氧糖酵解关键酶PKM2、LDHA表达下调,Lac生成减少,同时,NLRP3蛋白表达和炎症因子IL-1β、IL-18减少,表明PF可以抑制有氧糖酵解和NLRP3炎症小体激活,减轻炎症反应。LI等[38]研究表明,PF显著抑制了脓毒症急性肝损伤大鼠NLRP3炎症小体激活及炎症因子TNF-α、IL-1β和IL-18的表达。但PF调控有氧糖酵解,影响炎症反应的机制仍然不详。

3.4 PF通过抑制PI3K/AKT/HIF-1α信号通路,减轻LPS诱导的HK-2细胞的有氧糖酵解和炎症反应

为了进一步探究PF减轻有氧糖酵解的机制,本研究在PF干预基础上使用PI3K特异性激活剂740Y-P处理HK-2细胞。结果发现,有氧糖酵解关键酶PKM2、LDHA、终产物Lac的水平及ECAR反而升高;同时,NLRP3蛋白表达上调,炎症因子IL-1β、IL-18含量升高,表明740Y-P逆转了PF减轻有氧糖酵解及炎症反应的作用。此外,本研究还发现,LPS组通路蛋白p-PI3K、p-AKT、HIF-1α蛋白表达上调;给予PF处理后,p-PI3k、p-AKT、HIF-1α蛋白表达下调;经740Y-P处理后,通路蛋白p-PI3k、p-AKT、HIF-1α蛋白表达反而升高。因此,本研究认为PI3K/AKT/HIF-1α通路参与SA-AKI肾小管细胞损伤的体外模型有氧糖酵解和炎症反应的发生。

综上所述,PF减轻LPS诱导的HK-2细胞的有氧糖酵解和炎症反应,其机制是通过抑制PI3K/AKT/HIF-1α信号通路发挥作用。

利益冲突 本文所有作者声明不存在利益冲突

参考文献:

[1] POSTON J T, KOYNER J L. Sepsis associated acute kidney injury[J]. Br Med J, 2019: k4891. DOI:10.1136/bmj.k4891.

[2] BAGSHAW S M, LAPINSKY S, DIAL S, *et al*. Acute kidney injury in septic shock: clinical outcomes and impact of duration of hypotension prior to initiation of antimicrobial therapy[J]. Intensive Care Med, 2009, 35(5): 871-881. DOI:10.1007/s00134-008-1367-2.

[3] CHANG Y M, CHOU Y T, KAN W C, *et al*. Sepsis and acute kidney injury: a review focusing on the bidirectional interplay[J]. Int J Mol Sci, 2022, 23(16): 9159. DOI: 10.3390/ijms23169159.

[4] HELLMAN T, UUSALO P, JÄRVISALO M J. Renal replacement techniques in septic shock[J]. Int J Mol Sci, 2021, 22(19): 10238. DOI:10.3390/ijms221910238.

[5] LI C, WANG W, XIE S S, *et al*. The programmed cell death of macrophages, endothelial cells, and tubular epithelial cells in sepsis-AKI[J]. Front Med, 2021, 8: 796724. DOI: 10.3389/fmed.2021.796724.

[6] QIAO J, TAN Y, LIU H, *et al*. Histone H3K18 and ezrin lactylation promote renal dysfunction in sepsis-associated acute kidney injury[J]. Adv Sci (Weinh), 2024, 11(28): e2307216. DOI:10.1002/advs.202307216.

[7] PALSSON-MCDERMOTT E M, O'NEILL L A J. The Warburg effect then and now: From cancer to inflammatory diseases[J]. BioEssays, 2013, 35(11): 965-973. DOI: 10.1002/bies.201300084.

[8] BAR-OR D, CARRICK M, TANNER A 2nd, *et al*. Overcoming the Warburg effect: Is it the key to survival in sepsis?[J]. J Crit Care, 2018, 43: 197-201. DOI:10.1016/j.jcrc.2017.09.012.

[9] WALTZ P, CARCHMAN E, GOMEZ H, *et al*. Sepsis results in an altered renal metabolic and osmolyte profile[J]. J Surg Res, 2016, 202(1): 8-12. DOI:10.1016/j.jss.2015.12.011.

[10] TAN C Y, GU J, LI T, *et al*. Inhibition of aerobic glycolysis alleviates sepsis-induced acute kidney injury by promoting lactate/Sirtuin 3/AMPK-regulated autophagy[J]. Int J Mol Med, 2021. DOI:10.3892/ijmm.2021.4852.

[11] LIAO S, LIANG L, YUE C X, *et al*. CD38 is involved in cell energy metabolism *via* activating the PI3K/AKT/mTOR signaling pathway in cervical cancer cells[J]. Int J Oncol, 2020, 57(1): 338-354. DOI:10.3892/ijo.2020.5040.

[12] ZHANG T, ZHANG Y G, YANG Z H, *et al*. *Echinococcus multilocularis* protoscoleces enhance glycolysis to promote

M2 macrophages through PI3K/Akt/mTOR signaling pathway [J]. Pathog Glob Health, 2023, 117(4): 409-416. DOI: 10.1080/20477724.2022.2104055.

[13] MASOUD G N, LI W. HIF-1α pathway: role, regulation and intervention for cancer therapy[J]. Acta Pharm Sin B, 2015, 5(5): 378-389. DOI:10.1016/j.apsb.2015.05.007.

[14] CODO A C, DAVANZO G G, DE BRITO MONTEIRO L, *et al*. Elevated glucose levels favor SARS-CoV-2 infection and monocyte response through a HIF-1α/glycolysis-dependent axis[J]. Cell Metab, 2020, 32(3): 437-446.e5. DOI:10.1016/j.cmet.2020.07.007.

[15] XIE L P, ZHANG G Y, WU Y T, *et al*. Protective effects of Wenqingyin on sepsis-induced acute lung injury through regulation of the receptor for advanced glycation end products pathway[J]. Phytomedicine, 2024, 129: 155654. DOI:10.1016/j.phymed.2024.155654.

[16] LI R, SHI C R, WEI C T, *et al*. Fufang Shenhua tablet inhibits renal fibrosis by inhibiting PI3K/AKT [J]. Phytomedicine, 2023, 116: 154873. DOI: 10.1016/j.phymed.2023.154873.

[17] ZHENG Z B, MA H, ZHANG X, *et al*. Enhanced glycolytic metabolism contributes to cardiac dysfunction in polymicrobial sepsis[J]. J Infect Dis, 2017, 215(9): 1396-1406. DOI:10.1093/infdis/jix138.

[18] GAO M, HA T Z, ZHANG X, *et al*. Toll-like receptor 3 plays a central role in cardiac dysfunction during polymicrobial sepsis [J]. Crit Care Med, 2012, 40(8): 2390-2399. DOI:10.1097/CCM.0b013e3182535aeb.

[19] FENG Y, ZOU L, ZHANG M, *et al*. MyD88 and Trif signaling play distinct roles in cardiac dysfunction and mortality during endotoxin shock and polymicrobial sepsis [J]. Anesthesiology, 2011, 115 (3): 555-567. DOI: 10.1097/ALN.0b013e31822a22f7.

[20] ZOU L, FENG Y, CHEN Y J, *et al*. Toll-like receptor 2 plays a critical role in cardiac dysfunction during polymicrobial sepsis [J]. Crit Care Med, 2010, 38(5): 1335-1342. DOI:10.1097/CCM.0b013e3181d99e67.

[21] KRAWCZYK C M, HOLOWKA T, SUN J, *et al*. Toll-like receptor-induced changes in glycolytic metabolism regulate dendritic cell activation[J]. Blood, 2010, 115(23): 4742-4749. DOI:10.1182/blood-2009-10-249540.

[22] O'NEILL L A J, PEARCE E J. Immunometabolism governs dendritic cell and macrophage function [J]. J Exp Med, 2016, 213(1): 15-23. DOI:10.1084/jem.20151570.

[23] CHENG S C, SCICLUNA B P, ARTS R J W, *et al*. Broad defects in the energy metabolism of leukocytes underlie immunoparalysis in sepsis[J]. Nat Immunol, 2016, 17(4): 406-413. DOI:10.1038/ni.3398.

[24] NI D, LIN X F, DENG C H, *et al*. Energy metabolism: from physiological changes to targets in sepsis-induced cardiomyopathy[J]. Hellenic J Cardiol, 2024, 80: 96-106. DOI:10.1016/j.hjc.2024.05.010.

[25] LIU A B, TAN B, YANG P, *et al*. The role of inflammatory response and metabolic reprogramming in sepsis-associated acute kidney injury: mechanistic insights and therapeutic potential [J]. Front Immunol, 2024, 15: 1487576. DOI: 10.3389/fimmu.2024.1487576.

[26] LUO P, ZHANG Q, ZHONG T Y, *et al*. Celastrol mitigates inflammation in sepsis by inhibiting the PKM2-dependent Warburg effect[J]. Military Med Res, 2022, 9: 22. DOI: 10.1186/s40779-022-00381-4.

[27] ZHANG Q, LUO P, XIA F, *et al*. Capsaicin ameliorates inflammation in a TRPV1-independent mechanism by inhibiting PKM2-LDHA-mediated Warburg effect in sepsis [J]. Cell Chem Biol, 2022, 29(8): 1248-1259.e6. DOI: 10.1016/j.chembiol.2022.06.011.

[28] WANG H T, FAN C Y, CHEN X L, *et al*. Pyruvate kinase M2 nuclear translocation regulate ferroptosis-associated acute lung injury in cytokine storm [J]. Inflammation, 2024, 47 (5): 1667-1684. DOI: 10.1007/s10753-024-02000-x.

[29] POUYSSÉGUR J, MARCHIQ I, PARKS S K, *et al*. 'Warburg effect' controls tumor growth, bacterial, viral infections and immunity—Genetic deconstruction and therapeutic perspectives[J]. Semin Cancer Biol, 2022, 86 (Pt 2): 334-346. DOI:10.1016/j.semcancer.2022.07.004.

[30] HUANG P J, LIU J W. Simultaneous detection of L-lactate and D-glucose using DNA aptamers in human blood serum [J]. Angew Chem Int Ed, 2023, 62(12): e202212879. DOI:10.1002/anie.202212879.

[31] AN S, YAO Y, HU H B, *et al*. PDHA1 hyperacetylation-mediated lactate overproduction promotes sepsis-induced acute kidney injury *via* Fis1 lactylation[J]. Cell Death Dis, 2023, 14(7): 457. DOI:10.1038/s41419-023-05952-4.

[32] 雷娇, 张铭, 龚禹, 等. 基于网络药理学、分子对接及动物实验探讨芍药苷对脓毒症肠损伤的作用及机制[J]. 中国病理生理杂志, 2025, 41(3): 545-554. DOI:10.3969/j.issn.1000-4718.2025.03.015.
LEI J, ZHANG M, GONG Y, *et al*. Study on role and mechanism of paeoniflorin in septic intestinal injury based on network pharmacology, molecular docking and animal experi-ments[J]. Chin J Pathophysiol, 2025, 41(3): 545-554. DOI:10.3969/j.issn.1000-4718.2025.03.015.

[33] 金莹莹, 时乐, 郝永熙, 等. 芍药苷对雷西莫特诱导的巨噬细胞有氧糖酵解的影响[J]. 中国临床药理学杂志, 2024, 40(5): 683-687. DOI: 10.13699/j.cnki.1001-6821.

2024.05.011.
JIN Y Y, SHI L, HAO Y X, *et al*. Effect of paeoniflorin on aerobic glycolysis of macrophages induced by resiquimod [J]. Chin J Clin Pharmacol, 2024, 40(5): 683-687. DOI: 10.13699/j.cnki.1001-6821.2024.05.011.

[34] OLONA A, LEISHMAN S, ANAND P K. The NLRP3 inflammasome: regulation by metabolic signals[J]. Trends Immunol, 2022, 43(12): 978-989. DOI: 10.1016/j.it.2022.10.003.

[35] SHI X Y, TAN S C, TAN S P. NLRP3 inflammasome in sepsis (Review)[J]. Mol Med Rep, 2021, 24(1): 514. DOI:10.3892/mmr.2021.12153.

[36] LIU W Z, LIU T Y, ZHENG Y J, *et al*. Metabolic reprogramming and its regulatory mechanism in sepsis-mediated inflammation[J]. J Inflamm Res, 2023, 16: 1195-1207. DOI:10.2147/jir.s403778.

[37] WANG L, WANG D G, ZHANG T L, *et al*. The role of immunometabolism in macrophage polarization and its impact on acute lung injury/acute respiratory distress syndrome[J]. Front Immunol, 2023, 14: 1117548. DOI: 10.3389/fimmu.2023.1117548.

[38] LI L, WANG H, ZHAO S P, *et al*. Paeoniflorin ameliorates lipopolysaccharide-induced acute liver injury by inhibiting oxidative stress and inflammation *via* SIRT1/FOXO1a/SOD2 signaling in rats[J]. Phytother Res, 2022, 36(6): 2558-2571. DOI:10.1002/ptr.7471.

(收稿:2025-05-15;修回:2025-09-24)
(编辑 刘秋池)